

Piezoelectric MEMS-based wideband energy harvesting systems using a frequency-up-conversion cantilever stopper

Huicong Liu^a, Chengkuo Lee^{b,*}, Takeshi Kobayashi^c, Cho Jui Tay^a, Chenggen Quan^a

^a Department of Mechanical Engineering, National University of Singapore, 9 Engineering Drive 1, Singapore 117576, Singapore

^b Department of Electrical & Computer Engineering, National University of Singapore, 4 Engineering Drive 3, Singapore 117576, Singapore

^c National Institute of Advanced Industrial Science and Technology (AIST), 1-2-1 Namiki, Tsukuba, Ibaraki 305-8564, Japan

ARTICLE INFO

Article history:

Available online 15 February 2012

Keywords:

Microelectromechanical systems (MEMS)
Piezoelectric energy harvesting system
PZT cantilever
Wideband
Frequency-up-conversion (FUC)

ABSTRACT

Two MEMS-based piezoelectric energy harvesting (EH) systems with wideband operation frequency range and capability of converting random and low-frequency vibrations to high-frequency self-oscillations have been proposed. In the first EH system (EH-I), by incorporating a high-resonant-frequency (HRF) cantilever as a frequency-up-conversion (FUC) stopper, the vibration amplitude of a low-resonant-frequency (LRF) cantilever with a resonant frequency of 36 Hz is suppressed and the operation bandwidth is increased to 22 Hz at 0.8 g. The HRF cantilever is then triggered to vibrate at 618 Hz. In the second EH system (EH-II), by employing a straight cantilever as the FUC stopper, the operation frequency range of a meandered cantilever which responds to lower frequency vibration is further moved downward from 12 Hz to 26 Hz, and the voltage and power generation are significantly improved. The peak-power densities of the EH-II system are $61.5 \mu\text{W}/\text{cm}^3$ and $159.4 \mu\text{W}/\text{cm}^3$ operating at relatively lower operation frequencies of 20 Hz and 25 Hz at 0.8 g, respectively.

© 2012 Elsevier B.V. All rights reserved.

1. Introduction

Thin film piezoelectric lead zirconate titanate (PZT) materials offer a number of advantages in microelectromechanical systems (MEMS) as such devices provide large motions with low hysteresis in applications such as actuating mirrors [1], and raster scanning mirrors [2]. They also provide good signal-to-noise ratio in a wide dynamic range [3–7]. The piezoelectric coefficient of PZT is more superior than other piezoelectric thin films, such as ZnO and AlN, due to the high energy density. Hence, PZT thin films are good transducer materials for MEMS based energy harvesters [8–10].

Vibration-based MEMS energy harvesters have received increasing attention as a potential power source for microelectronics and wireless sensor nodes [11,12]. To date most energy harvesters based on piezoelectric, electromagnetic and electrostatic transduction mechanisms, particularly MEMS-based harvesters, operate at frequencies of more than 100 Hz [13–17]. Increasing compliant spring and bulk movable mass are required to achieve lower resonant frequency. It is a great challenge to realize small size and low resonant frequency at the same time due to the limitation of microfabrication processes and brittle properties of silicon material. The generated power

is theoretically proportional to the cube of the operation frequency and drops dramatically at low frequencies [18]. Thus energy harvesters with low resonant frequencies would result in reduced power output. However, harvesting energy from low frequency vibrations, such as human motions (<10 Hz), vehicle (<20 Hz) and machine vibrations (<50 Hz) [19–21] is desirable in applications such as implantable electronic devices and wireless sensor nodes. Thus FUC approach has been touted as a breakthrough to boost output power at low vibration frequencies [22].

Several researchers have developed FUC energy harvesters by utilizing magnetic forces [23,24]. In this approach, a magnet attached to a low-frequency or bulked diaphragm resonantly or non-resonantly catches and releases magnetic strips mounted on high-frequency oscillators, resulting in self-oscillations of the oscillators. These methods require additional magnets to generate current and are suitable for electromagnetic energy harvesters. Jung et al. [25] demonstrated a shock-based FUC approach using a buckled elastic beam integrated with high-frequency piezoelectric cantilevers. A sudden acceleration change introduced by the buckled beam would excite the self-oscillations of the piezoelectric cantilevers. However, this method requires large accelerations to drive the buckled beam. Renaud et al. [26] has reported a non-resonant impact-based energy harvester driven by a free ball moving in a guided channel where top and bottom piezoelectric benders are mounted in between. The method however does not benefit from the power enhancement of a resonant operation. A

* Corresponding author. Tel.: +65 6516 5865; fax: +65 6779 1103.
E-mail address: elelc@nus.edu.sg (C. Lee).

resonant impact-based energy harvesting prototype which utilizes a low-frequency resonator to directly impact two high-frequency PZT bimorphs in order to trigger their self-oscillations and generate power at high operation frequencies was also reported by Gu et al. [27]. The prototype suffered from large device size and has not been realized by MEMS technology. In fact, none of the aforementioned works use micro-scale approaches [25–26].

For a given acceleration, the vibration amplitude of an oscillator is inversely proportional to the square of the vibration frequency. A lower resonant frequency requires an increased displacement space and mechanical stoppers to prevent damage of the oscillator, thus reducing the generated power density of the device, though the mechanical stopper does broaden the frequency bandwidth [28,29]. In this work, instead of increasing the extra space to accommodate the displacement of the LRF oscillator, we incorporate a piezoelectric HRF cantilever which is excited into self-oscillation by the impact of the LRF cantilever and at the same time acts as an energy harvester. This will not only reduce the device space and protect the oscillator, but also realize a wide operation band and FUC behavior. As a result, additional significant power will be generated and power density of the system will be improved.

2. Working principle

Fig. 1(a) and (b) shows the architecture and schematic model of a vibration-based wideband EH system assembled with FUC stopper. The system contains an excitation oscillator with stiffness k_0 , damping coefficient c_0 , and proof mass m_0 . Another oscillator which acts as a FUC stopper is placed at a distance of x_0 above the excitation oscillator, with stiffness k_1 , damping coefficient c_1 and proof mass m_1 . The resonant frequency and the spring stiffness of the FUC oscillator are larger while the proof mass is smaller than that of the excitation oscillator. The operation mechanism is outlined in Fig. 1(c). The differential equation of the motion of the wideband EH system with cantilever stopper engaged can be written as

$$\begin{cases} (m_0 + m_1)\ddot{z} + (c_0 + c_1)\dot{z} + (k_0 + k_1)z - k_1x_0 = -(m_0 + m_1)\ddot{y} & (z \geq x_0) \\ m_0\ddot{z} + c_0\dot{z} + k_0z = -m_0\ddot{y} & (z < x_0) \end{cases} \quad (1)$$

When the vibration amplitude of the excitation oscillator is less than x_0 , the stiffness of the oscillator remains as k_0 . When the vibration amplitude exceeds x_0 , the excitation oscillator would engage the FUC oscillator, resulting in a sudden change in the effective stiffness (from k_0 to $k_0 + k_1$) and the effective mass (from m_0 to $m_0 + m_1$). Since $m_1 \leq m_0$ and $k_1 \geq k_0$, the effective resonant frequency is increased accordingly. Such increment enables the resonance of the excitation oscillator to broaden over a wider frequency range [30]. When the excitation oscillator moves away from the FUC oscillator, the FUC oscillator would vibrate at its own resonant frequency, which is much higher than the excitation frequency. Thus broadening of the frequency wideband and FUC behavior are achieved simultaneously.

The analytical model of a wideband energy harvester using stopper has been built and analyzed by Soliman et al. [31,32] and Liu et al. [29], which is applicable to our proposed EH systems. Based on the analytical model, it is found that the key parameters affected on the frequency wideband behavior include input acceleration, damping coefficient, effective stiffness and gap distance. The frequency wideband behavior of the system is strengthened by an increase in the effective stiffness and a decrease in the damping coefficient. However, the practical situation is that higher stiffness will also induce higher damping coefficient of the structure. Normally it is impossible to increase the effective stiffness of the system and decrease the damping of the FUC stopper at the same time.

According to our experiments, if the resonant frequency of the excitation oscillator is below 50 Hz, the resonant frequency of the FUC stopper should be around 5–10 times higher. In addition, a high acceleration is also preferred to realize a better performance (wider operating bandwidth and higher power output). There is a trade-off for the gap distance, since it affects the frequency bandwidth and output voltage with opposite trend.

3. Device configurations

3.1. EH-I system

As shown in Fig. 2(a), the proposed wideband EH-I system contains a low-resonant-frequency energy harvesting cantilever (denoted as LRF cantilever) and a high-resonant-frequency energy harvesting cantilever (denoted as HRF cantilever). The LRF cantilever as shown in Fig. 2(b) comprises of a silicon supporting beam ($3 \text{ mm} \times 5 \text{ mm} \times 5 \text{ }\mu\text{m}$) deposited with a PZT layer and silicon inertial mass ($5 \text{ mm} \times 5 \text{ mm} \times 0.4 \text{ mm}$). The PZT layer consists of 10 PZT stripes electrically isolated from one another. The HRF cantilever (Fig. 2(c)) has similar dimensions and configuration with that of the LRF cantilever, but without an inertial mass. The resonant frequencies of the LRF and HRF cantilevers are 36 Hz and 618 Hz, respectively. Figs. 2(d) and (e) illustrate the vibration behavior of the wideband EH-I system. The LRF and HRF cantilevers are assembled with a pre-determined stop-spacing of 1 mm. The vibration amplitude of the LRF cantilever is larger than the stop-spacing and it is able to respond to ambient vibrations nearby its resonant frequency and further extend over a wider frequency bandwidth by the HRF cantilever which acts as a FUC stopper. In the meantime, the HRF cantilever is triggered by the inertial mass of the LRF cantilever into a high frequency self-oscillation. Due to the piezoelectric effect, the electric current is generated once the PZT layer on both LRF and HRF cantilevers deform.

The advantages in employing the HRF cantilever as a FUC stopper are that it protects the excitation oscillator from damage during vibration and broadens the operation range. The system also converts ambient low frequency vibration to a high frequency self-oscillation. Using MEMS technology, the proposed system is applied to a piezoelectric-based EH system by the use of cantilever beams deposited with piezoelectric PZT material. To further improve the effectiveness of the FUC stopper, as well as reduce the device size and operation frequency, a wideband EH-II system is developed.

3.2. EH-II system

As illustrated in Fig. 3(a), the LRF cantilever used in wideband EH-I system is replaced by a meandered cantilever with a smaller chip size ($5.2 \text{ mm} \times 4.2 \text{ mm}$) in the proposed EH-II system. The HRF cantilever is replaced by a straight cantilever of the same size. A cross-sectional view of the EH-II system is shown in Fig. 3(b). The meandered cantilever as shown in Fig. 3(c) consists of a double-S-shaped silicon beam coated with PZT thin film layer and a silicon mass ($2 \text{ mm} \times 1.65 \text{ mm} \times 0.4 \text{ mm}$) at its end. It is not only smaller in size but also has a lower resonant frequency of 20 Hz as well. The straight cantilever which has a relatively higher resonant frequency of 127 Hz has a rectangular silicon beam and a mass at its end and a PZT layer is also coated on the silicon beam. The PZT layer deposited on the meandered cantilever is limited and the operation frequency is low, hence the power generated by the meandered cantilever would be extremely small. However, due to the low stiffness of the beam, its vibration amplitude is relatively large. Hence, with the large vibration amplitude, the meandered cantilever is able to convert its low-frequency vibration into a high-frequency oscillation of the straight cantilever after impact and increase the total output power significantly.

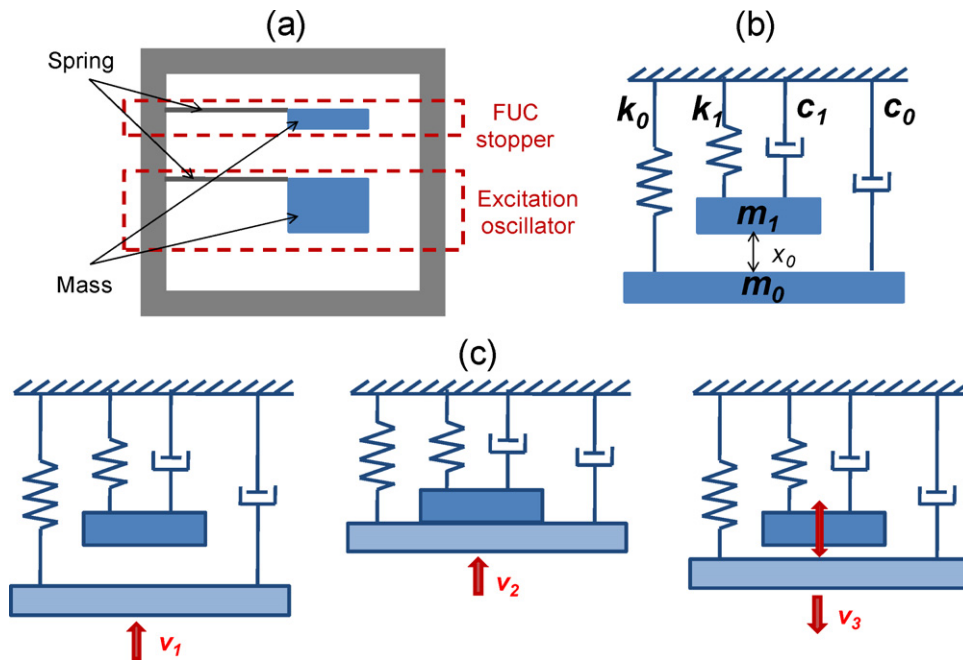


Fig. 1. (a) Architecture, (b) schematic model and (c) operation mechanism of a vibration-based wideband EH system with FUC stopper.

4. Results and discussion

4.1. EH-I system

In this experimental configuration of EH-I system, 2 PZT stripes of both the LRF and HRF cantilevers are selected and connected in series for the energy harvesting measurement. Fig. 4(a) shows the output voltage of the LRF cantilever against the sweeping frequencies under different input accelerations. As the input acceleration increases from 0.1 g to 0.4 g, the output voltage initially shows a peak value of 50 mV at 36 Hz and gradually increases to 52 mV at 32 Hz and 77 mV at 43 Hz which indicates a bandwidth broadening behavior. At 0.8 g, the operation bandwidth is widened to 22 Hz, while the voltage output steadily increases from 50 mV at 30 Hz to 102 mV at 52 Hz. Beyond 52 Hz, the output voltage drops dramatically to a low level. This is due to the change of the system to an unstable state. The peak-power spectra of the LRF cantilever

against frequency at the corresponding accelerations of 0.1 g, 0.4 g and 0.8 g are plotted in Fig. 4(b). At input acceleration of 0.8 g, the peak-power output increases gradually from 0.003 μ W at 30 Hz to 0.012 μ W at 52 Hz.

For an input acceleration of 0.8 g, Fig. 5(a) and (b) shows instantaneous output voltages of the LRF and HRF cantilevers at 37 Hz and 51 Hz, respectively. In Fig. 5(a), the output voltage of the LRF cantilever (in blue) oscillates at 37 Hz; when it engages the FUC stopper, i.e., the HRF cantilever, it (in red) starts to self-oscillate at its first resonant frequency of 618 Hz, at an average peak-voltage of 73 mV, which is higher than the average peak-voltage of the LRF cantilever of 65.5 mV. At a frequency of 51 Hz (Fig. 5(b)), the average peak-voltage for the LRF cantilever is 87.2 mV, while the average peak-voltage for the HRF cantilever is increased to 106.1 mV at a self-oscillating frequency of 618 Hz.

The instantaneous output power spectra at the corresponding frequencies of 37 Hz and 51 Hz at 0.8 g are approximately

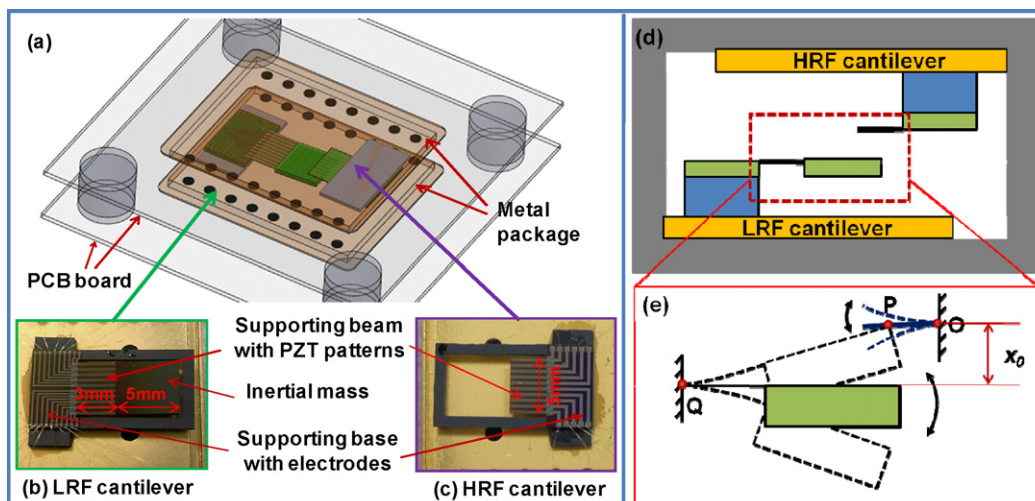


Fig. 2. (a) Schematic drawing of EH-I system; (b) fabricated LRF cantilever; (c) fabricated HRF cantilever; (d) arrangement and (e) vibration behavior illustration of EH-I system.

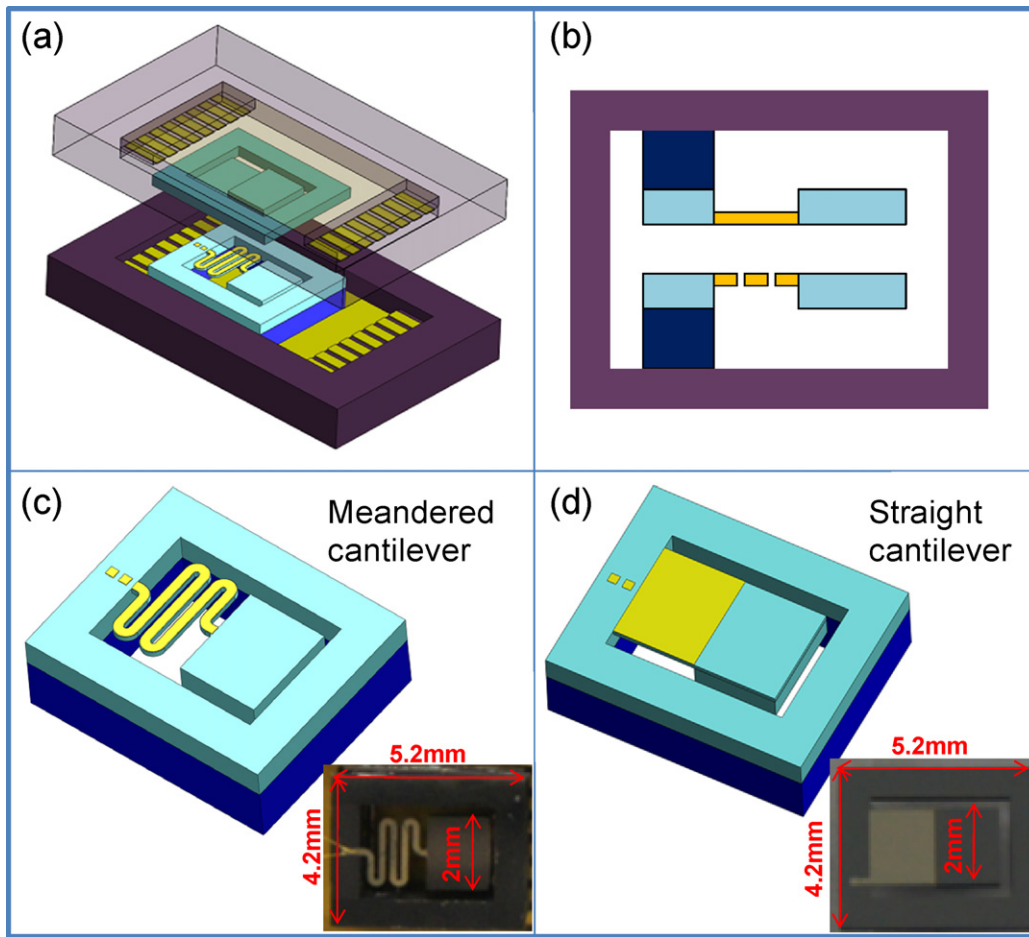


Fig. 3. (a) Schematic and (b) cross section of EH-II system; (c) fabricated meandered cantilever; (d) fabricated straight cantilever.

0.006 μW and 0.012 μW , respectively. The corresponding average peak-power of the LRF cantilever with 10 PZT stripes would expect to be around 0.03 μW and 0.06 μW , respectively. As for the HRF cantilever, the average peak-power at 37 Hz and 51 Hz are around 0.018 μW and 0.026 μW . Hence, the average peak-power of the HRF cantilever with 10 PZT strips would expect to be around 0.09 μW and 0.13 μW . The above results show that by incorporating the FUC stopper, the total peak-power of the system at input acceleration of 0.8 g is increased to 0.12 μW and 0.19 μW at 37 Hz and 51 Hz, respectively.

4.2. EH-II system

From the instantaneous output voltage spectra of EH-II system, it is found that FUC occurs during a wide operation frequency which ranges from 12 Hz to 26 Hz for an input acceleration of 0.8 g. Fig. 6

shows the instantaneous output voltages of the meandered and straight cantilevers at vibration frequencies of 20 Hz and 25 Hz. In Fig. 6(a), the meandered cantilever (indicated in green) which oscillates at 20 Hz impacts and releases the straight cantilever (FUC stopper) at every vibration cycle and results in a self-oscillation of the straight cantilever at 127 Hz (indicated in purple). The average peak-voltage of the straight cantilever of 153 mV is about 5 times higher than that of the meandered cantilever. Likewise, in Fig. 6(b), the average peak-voltage of the meandered cantilever oscillating at 25 Hz is 209 mV, while that of the straight cantilever which oscillates at 127 Hz has an average peak-voltage of 49 mV.

It is seen in Fig. 7 that at frequencies of 20 Hz and 25 Hz and assuming that the load resistance matches with internal impedances, optimal power spectra can be calculated from the corresponding output voltages shown in Fig. 6. For the meandered cantilever, the average peak-power obtained is in the range of

Table 1 Comparison of EH-I and EH-II systems.

	EH-I system			EH-II system		
		LRF cantilever	HRF cantilever		Meandered cantilever	Straight cantilever
Peak-power (μW)	37 Hz	0.03	0.09	20 Hz	0.003	0.34
	51 Hz	0.06	0.13	25 Hz	0.01	0.87
Cantilever size (mm^3)		$8 \times 5 \times 0.4$	$3 \times 5 \times 0.01$		$3.45 \times 2 \times 0.4$	$3.45 \times 2 \times 0.4$
Peak-power density ($\mu\text{W}/\text{cm}^3$)	37 Hz	7.4		20 Hz	61.5	
	51 Hz	11.8		25 Hz	159.4	
Resonant frequency (Hz)		36			20	
Operation bandwidth (Hz)		22 (30–52)			14 (12–26)	

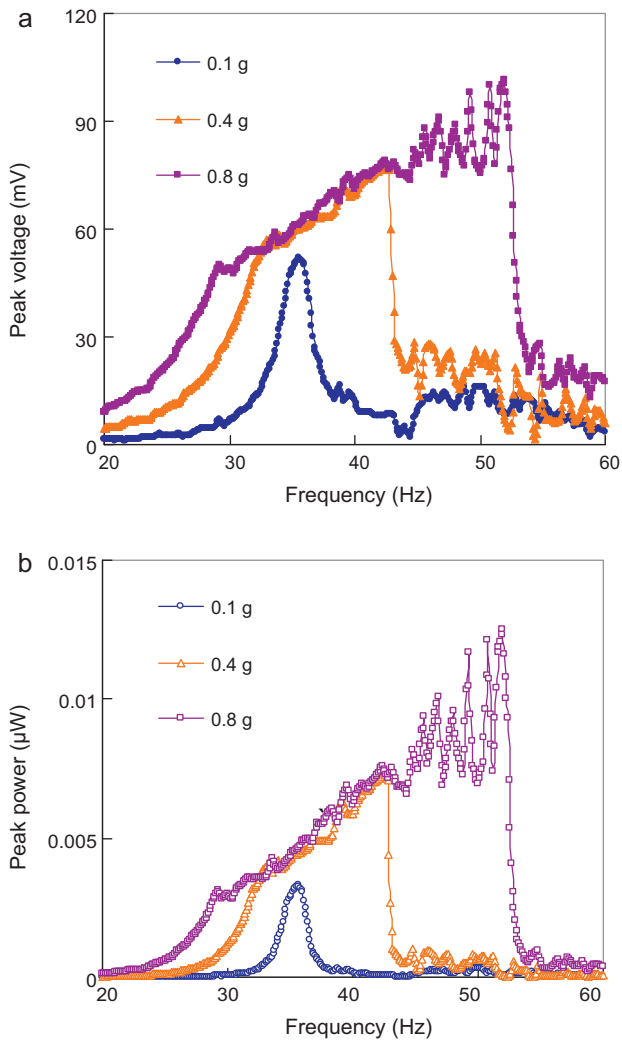


Fig. 4. (a) Output peak-voltage and (b) peak-power of the LRF cantilever with different input accelerations.

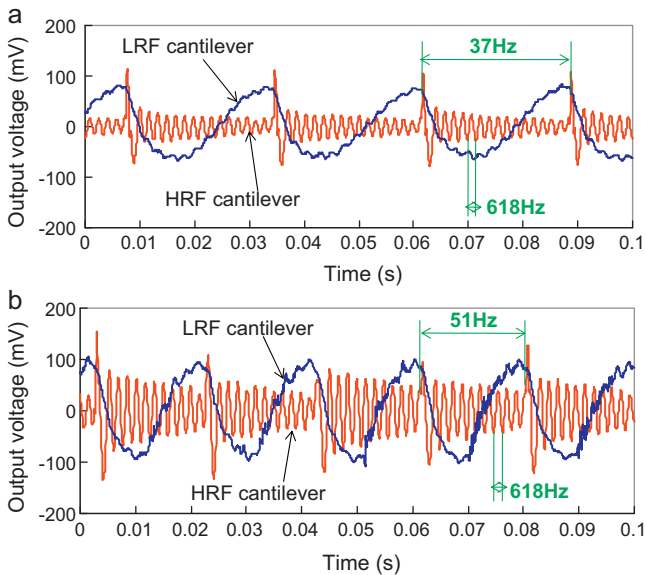


Fig. 5. Instantaneous output voltages of LRF and HRF cantilevers at frequencies of (a) 37 Hz and (b) 51 Hz.

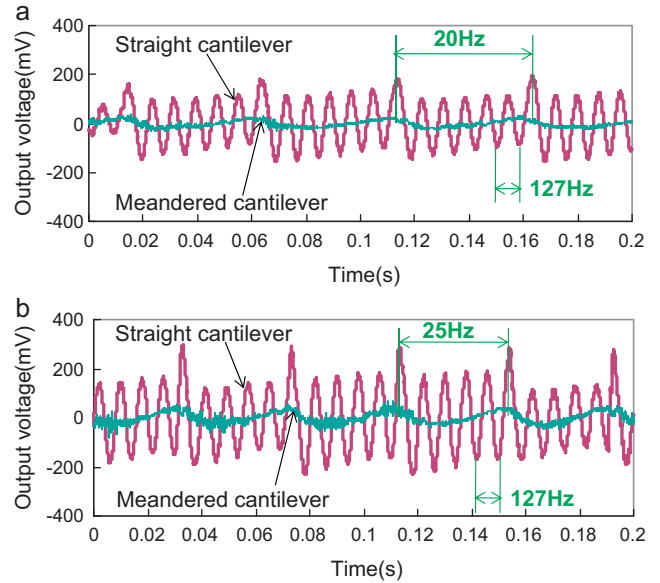


Fig. 6. Instantaneous output voltages of meandered and straight cantilevers at frequencies of (a) 20 Hz and (b) 25 Hz.

0.003 μ W to 0.01 μ W. While that of the straight cantilever ranges from 0.34 μ W to 0.87 μ W. As can be seen, the average peak-power of the straight cantilever is up to 100 times higher than that of the meandered cantilever. With regards to the rms output power, the straight cantilever is able to deliver up to 200 times that of the

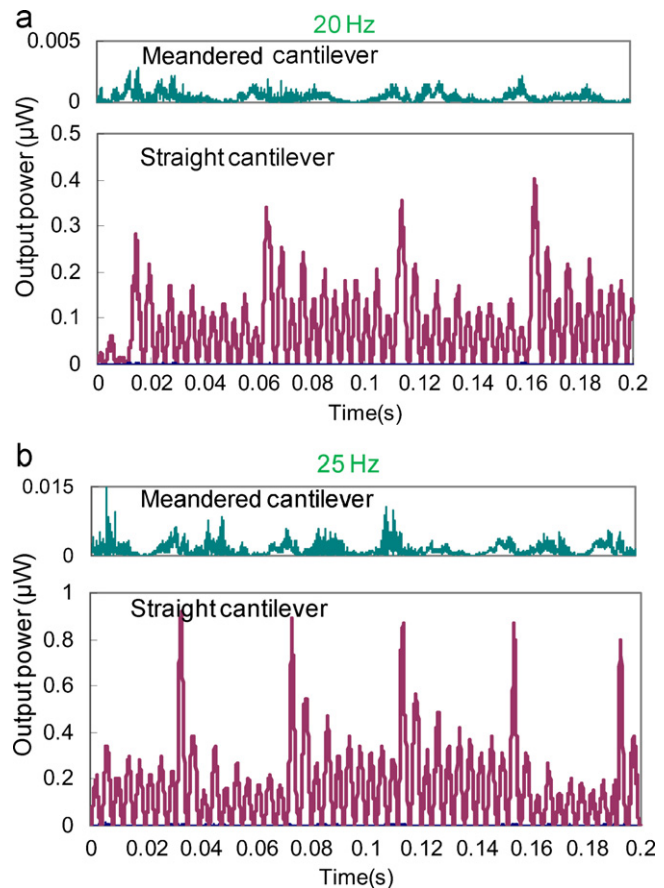


Fig. 7. Instantaneous output power spectra of meandered and straight cantilevers at frequencies of (a) 20 Hz and (b) 25 Hz.

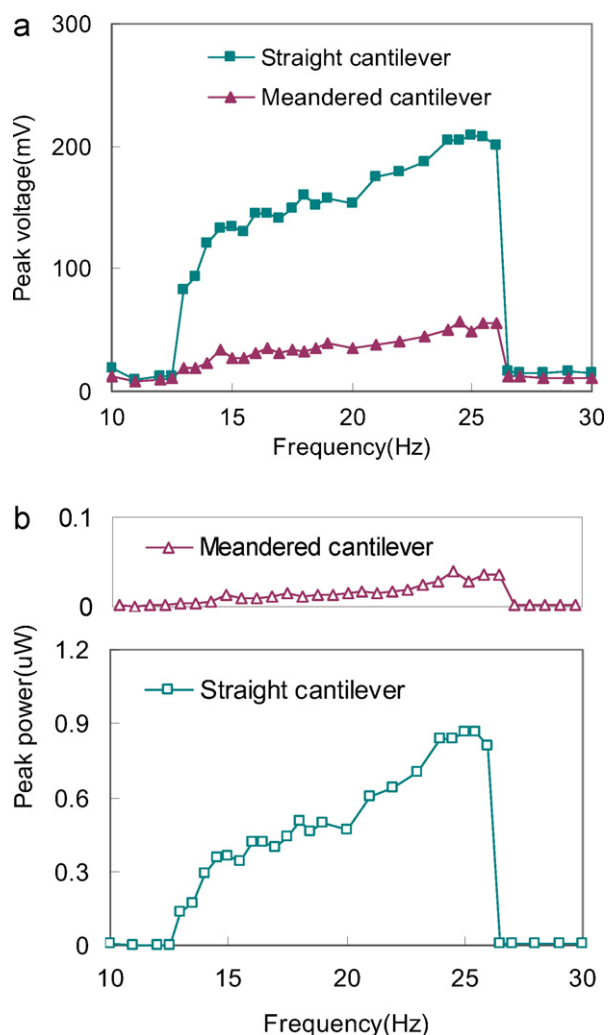


Fig. 8. (a) Average peak-voltage and (b) peak-power of meandered and straight cantilevers against frequencies from 10 Hz to 30 Hz at 0.8 g.

meandered cantilever. The significant boost of the output power is due to the FUC mechanism, which converts a low frequency vibration of the meandered cantilever into a high frequency vibration of the straight cantilever. In addition, the piezoelectric impedance of the straight cantilever of $96\text{ K}\Omega$ is significantly lower than that of the meandered cantilever of $1.5\text{ M}\Omega$. Hence the straight cantilever would have lower internal power consumption and higher effective power output.

The average peak-voltage and peak-power of the meandered and straight cantilevers at frequencies ranging from 10 Hz to 30 Hz and an acceleration of 0.8 g are shown in Fig. 8. As can be seen, significant output improvement in the straight cantilever is observed only after the meandered cantilever engages the straight cantilever at frequency range of 12 Hz to 26 Hz. At excitation frequencies of below 12 Hz and above 26 Hz, the insignificant voltage and power outputs of both cantilevers are due to the low vibration amplitude of the meandered cantilever which is insufficient to trigger the oscillation of the straight cantilever.

Table 1 shows a summary of the performance of the proposed EH-I and EH-II systems in terms of peak-power density (peak-power divided by the volume of the cantilever) and operation bandwidth. It is seen that when compared with EH-I system, the proposed EH-II system is able to achieve a much higher peak-power density of up to $159.4\text{ }\mu\text{W}/\text{cm}^3$ at a relatively low frequency of 25 Hz. In addition, the EH-II system has extended the operation

bandwidth by 14 Hz (from 12 Hz to 26 Hz) and operating frequency range is near the vibration frequency of human motion (10 Hz). This is an obvious advantage as currently there are still no reports of MEMS-based piezoelectric energy harvesters which operate at such low frequency.

5. Conclusions

We have proposed two wideband MEMS-EH systems with a FUC cantilever stopper for converting random and low-frequency external vibrations to self-oscillation of a FUC stopper at high resonant frequency. The main advantage of the proposed device is that it broadens the operation frequency range and increases the output voltage and power. The proposed EH-II system improves the power generation efficiency and operation frequency bandwidth limitation. The results obtained offer a possible solution for practical applications in low frequency situation such as that of human motion.

Acknowledgements

This work was partially supported by in research grant of MOE Tier-2 Academic Research Committee (ARC) Fund MOE2009-T2-2-011 (R-263000598112) and Faculty Research Committee (FRC) Grant (R-263-000-692-112) at the National University of Singapore.

References

- [1] C. Lee, F.-L. Hsiao, T. Kobayashi, K.H. Koh, P.V. Ramana, W. Xiang, B. Yang, C.W. Tan, D. Pinjala, A 1-V operated MEMS variable optical attenuator using piezoelectric PZT thin film actuators, *IEEE J. Selected Topics Quantum Electron.* 15 (5) (2009) 1529–1536.
- [2] Y. Yasuda, M. Akamatsu, M. Tani, T. Iijima, H. Toshiyoshi, Piezoelectric 2D optical micro scanners with PZT thick films, *Integr. Ferroelectr.* 76 (1) (2005) 81–91.
- [3] C. Lee, T. Itoh, G. Sasaki, T. Suga, Sol-gel derived PZT force sensor for scanning force microscopy, *Mater. Chem. Phys.* 44 (1) (1996) 25–29.
- [4] J. Chu, T. Itoh, C. Lee, T. Suga, K. Watanabe, Novel high vacuum scanning force microscope using a piezoelectric cantilever and phase detection method, *J. Vac. Sci. Technol. B* 15 (4) (1997) 1551–1555.
- [5] C. Lee, T. Itoh, T. Ohashi, R. Maeda, T. Suga, Development of a piezoelectric self-excitation and self-detection mechanism in PZT microcantilevers for dynamic scanning force microscopy in liquid, *J. Vac. Sci. Technol. B* 15 (4) (1997) 1559–1563.
- [6] L.-P. Wang, R.A. Wolf, Y. Wang Jr., K.K. Deng, L. Zou, R.J. Davis, S. Trolrier-McKinstry, Design, fabrication, and measurement of high-sensitivity piezoelectric microelectromechanical systems accelerometers, *IEEE J. Microelectromech. Syst.* 12 (4) (2003) 433–439.
- [7] Y. Cui, H. Meng, J. Wang, W. Dong, L. Wang, Deposition and sensing properties of PT/PZT/PT thin films for microforce sensors, *Phys. Scr. T209* (2007) 209–212.
- [8] Y.B. Jeon, R. Sood, J.H. Jeong, S.G. Kim, MEMS power generator with transverse mode thin film PZT, *Sens. Actuators A: Phys.* 122 (1) (2005) 16–22.
- [9] H.B. Fang, J.Q. Liu, Z.Y. Xu, L. Dong, L. Wang, D. Chen, B.C. Cai, Y. Liu, Fabrication and performance of MEMS-based piezoelectric power generator for vibration energy harvesting, *Microelectron. J.* 37 (11) (2006) 1280–1284.
- [10] J.C. Park, J.Y. Park, Y.P. Lee, Modeling and characterization of piezoelectric d33-mode MEMS energy harvester, *J. Microelectromech. Syst.* 19 (5) (2010) 1215–1222.
- [11] P.D. Mitcheson, E.M. Yeatman, G.K. Rao, A.S. Holmes, T.C. Green, Energy harvesting from human and machine motion for wireless electronic devices, *Proc. IEEE* 96 (9) (2008) 1457–1486.
- [12] B. Yang, J. Liu, G. Tang, J. Luo, C. Yang, Y. Li, A generator with nonlinear spring oscillator to provide vibrations of multi-frequency, *Appl. Phys. Lett.* 99 (22) (2011) 223505.
- [13] R. Elfrink, T.M. Kamel, M. Goedbloed, S. Matova, D. Hohlfeld, Y. van Andel, R. van Schaijk, Vibration energy harvesting with aluminum nitride-based piezoelectric devices, *J. Micromech. Microeng.* 19 (9) (2009) 094005.
- [14] D. Shena, J.-H. Parka, J.H. Noha, S.-Y. Choeb, S.-H. Kimc, H.C. Wikle III, D.-J. Kim, Micromachined PZT cantilever based on SOI structure for low frequency vibration energy harvesting, *Sens. Actuators A: Phys.* 154 (1) (2009) 103–108.
- [15] Y. Jiang, S. Masaoka, T. Fujita, M. Uehara, T. Toyonaga, K. Fujii, K. Higuchi, K. Maenaka, Fabrication of a vibration-driven electromagnetic energy harvester with integrated NdFeB/Ta multilayered micro-magnets, *J. Micromech. Microeng.* 21 (9) (2011) 095014.
- [16] F. Khan, F. Sassani, B. Stoeber, Copper foil-type vibration-based electromagnetic energy harvester, *J. Micromech. Microeng.* 20 (10) (2010) 125006.

- [17] L.G.W. Tvedt, D.S. Nguyen, E. Halvorsen, Nonlinear behavior of an electrostatic energy harvester under wide- and narrowband excitation, *J. Microelectromech. Syst.* 19 (2) (2009) 305–316.
- [18] S.P. Beeby, M.J. Tudor, N.M. White, Energy harvesting vibration sources for microsystems applications, *Meas. Sci. Technol.* 17 (12) (2006) 175–195.
- [19] S. Roundy, P.K. Wright, J. Rabaey, A study of low level vibrations as a power source for wireless sensor nodes, *Comput. Commun.* 26 (11) (2003) 1131–1144.
- [20] D. Paci, M. Schipani, V. Bottarel, D. Miatton, Optimization of a piezoelectric energy harvester for environmental broadband vibrations, in: *Proc. 15th IEEE ICECS*, 2008, pp. 177–181.
- [21] L.M. Miller, E. Halvorsen, T. Dong, P.K. Wright, Modeling and experimental verification of low-frequency MEMS energy harvesting from ambient vibrations, *J. Micromech. Microeng.* 21 (4) (2011) 045029.
- [22] H. Kulah, K. Najafi, Energy scavenging from low-frequency vibrations by using frequency up-conversion for wireless sensors applications, *IEEE Sens. J.* 8 (3) (2008) 261–268.
- [23] I. Sari, T. Balkan, H. Kulah, An electromagnetic micro power generator for low-frequency environmental vibrations based on the frequency up conversion technique, *J. Microelectromech. Syst.* 19 (1) (2010) 14–27.
- [24] T. Galchev, H. Kim, K. Najafi, Micro power generator for harvesting low-frequency and nonperiodic vibrations, *J. Microelectromech. Syst.* 20 (4) (2011) 852–866.
- [25] S.-M. Jung, K.-S. Yuna, Energy-harvesting device with mechanical frequency-up conversion mechanism for increased power efficiency and wideband operation, *Appl. Phys. Lett.* 96 (11) (2010) 11906.
- [26] M. Renaud, P. Fiorini, R. van Schaijk, C. van Hoof, Harvesting energy from the motion of human limb: the design and analysis of an impact-based piezoelectric generator, *Smart Mater. Struct.* 18 (3) (2009) 035001.
- [27] L. Gu, C. Livermore, Impact-driven, frequency up-converting coupled vibration energy harvesting device for low frequency operation, *Smart Mater. Struct.* 20 (4) (2011) 045004.
- [28] H. Liu, C.J. Tay, C. Quan, T. Kobayashi, C. Lee, Piezoelectric MEMS energy harvester for low-frequency vibrations with wideband operation range and steadily increased output power, *J. Microelectromech. Syst.* 20 (5) (2011) 1131–1142.
- [29] H. Liu, C. Lee, T. Kobayashi, C.J. Tay, C. Quan, Investigation of MEMS piezoelectric energy harvester system with frequency-widen-bandwidth mechanism introduced by mechanical stopper, *Smart mater. Struct.* 21 (3) (2012) 035005.
- [30] A. Narimani, M.F. Golnaraghi, G.N. Jazar, Frequency response of a piecewise linear vibration isolator, *J. Vib. Control* 10 (12) (2004) 1775–1794.
- [31] M.S.M. Soliman, E.M. Abdel-Rahman, E.F. El-Saadany, R.R. Mansour, A wide-band vibration-based energy harvester, *J. Micromech. Microeng.* 18 (11) (2008) 115021.
- [32] M.S.M. Soliman, E.M. Abdel-Rahman, E.F. El-Saadany, R.R. Mansour, A design procedure for wideband micropower generators, *J. Microelectromech. Syst.* 18 (6) (2009) 1288–1299.

Biographies

Huicong Liu received her B.S. and M.S. degrees in Department of Mechanical Engineering from University of Science and Technology Beijing, China, in 2006 and 2008, respectively. She is currently a PhD student in the Department of Mechanical Engineering, National University of Singapore. Her research interests are the dynamic characterization of MEMS components, mainly on vibration-based MEMS energy harvesters.

Chengkuo Lee received the M.S. degree in Materials Science and Engineering from National Tsing Hua University, Hsinchu, Taiwan, in 1991, the M.S. degree in

industrial and system engineering from Rutgers University, New Brunswick, NJ, in 1993, and the Ph.D. degree in precision engineering from The University of Tokyo, Tokyo, Japan, in 1996. He worked as a Foreign Researcher in the Nanometer-scale Manufacturing Science Laboratory of the Research Center for Advanced Science and Technology, The University of Tokyo, from 1993 to 1996. He had also worked in the Mechanical Engineering Laboratory, AIST, MITI of Japan as a JST Research Fellow in 1996. Thereafter, he became a Senior Research Staff Member of the Microsystems Laboratory, Industrial Technology Research Institute, Hsinchu, Taiwan. In September 1997, he joined Metrodyne Microsystem Corporation, Hsinchu, Taiwan, and established the MEMS device division and the first micromachining fab for commercial purposes in Taiwan. He was the Manager of the MEMS device division between 1997 and 2000. He was an Adjunct Assistant Professor in the Electro-physics Department of National Chiao Tung University, Hsinchu, Taiwan, in 1998, and an Adjunct Assistant Professor in the Institute of Precision Engineering of National Chung Hsing University, Taichung, Taiwan, from 2001 to 2005. In August 2001, he cofounded Asia Pacific Microsystems, Inc. (APM), where he first became Vice President of R&D, before becoming Vice President of the optical communication business unit and Special Assistant to the Chief Executive Officer in charge of international business and technical marketing for the MEMS foundry service. From 2006 to 2009, he was a Senior Member of the Technical Staff at the Institute of Microelectronics, A-Star, Singapore. He has been an Assistant Professor in the Department of Electrical and Computer Engineering, National University of Singapore, Singapore, since December 2005. He is the coauthor of *Advanced MEMS Packaging* (McGraw-Hill, 2010). He has contributed to more than 150 international conference papers and extended abstracts and 100 peer-reviewed international journal articles in the fields of Sensors, Actuators, Energy Harvesting, MEMS, NEMS, nanophotonics, and nanotechnology. He is also the holder of nine U.S. patents.

Takeshi Kobayashi received his B.S. and M.S. degree in Materials Science from The University of Tokyo. He also received Ph.D degree in Materials Science from The University of Tokyo in 2002. He worked as researcher in National Institute of Advance Industrial Science and Technology (AIST), Japan. His research interest includes piezoelectric MEMS devices and their application to wireless sensor network. He has contributed to 40 international journal papers and 40 conference proceedings. Two of his recent publications have been selected as high-lighted paper of *Journal of Micromechanics and Microengineering* in 2007 and 2008.

Cho Jui Tay is currently an associate professor at the National University of Singapore. His research interests include experimental mechanics, optical techniques and MEMS/NEMS. He has published widely in international journals and has coauthored and edited several book and book chapters. He has been involved in various editorial works and serves as a reviewer for 13 international journals and grant award agencies. He has delivered invited talks at various universities and research institutions. He holds several patents in the area of micro-components fabrication. He has won several research and best paper awards including the David Cargill Prize, United Kingdom.

Chenggen Quan graduated in 1982 from Harbin Institute of Technology (HIT), China, with a BEng degree in mechanical engineering. He received his MEng degree in optical engineering from HIT in 1988 and his PhD from Warwick University, UK, in 1992. His PhD research involved the quantitative analysis of holographic interferograms using fast Fourier transform algorithms. Before joining National University of Singapore (NUS) he worked as a senior engineer at National Measurement Centre, Singapore Productivity and Standards Board. He is currently an associate professor in the Department of Mechanical Engineering, NUS. His research interests include laser-based measurement techniques, nondestructive testing, optical shape measurement, moiré interferometry for electronic packaging, and automatic fringe-pattern analysis.